

Search for Charged Higgs Bosons Decaying into Top and Bottom Quarks in $p\bar{p}$ Collisions

V. M. Abazov,³⁶ B. Abbott,⁷⁵ M. Abolins,⁶⁵ B. S. Acharya,²⁹ M. Adams,⁵¹ T. Adams,⁴⁹ E. Aguilo,⁶ M. Ahsan,⁵⁹ G. D. Alexeev,³⁶ G. Alkhalaf,⁴⁰ A. Alton,^{64,*} G. Alverson,⁶³ G. A. Alves,² M. Anastasoia,³⁵ L. S. Ancu,³⁵ T. Andeen,⁵³ S. Anderson,⁴⁵ B. Andrieu,¹⁷ M. S. Anzels,⁵³ M. Aoki,⁵⁰ Y. Arnoud,¹⁴ M. Arov,⁶⁰ M. Arthaud,¹⁸ A. Askew,⁴⁹ B. Åsman,⁴¹ A. C. S. Assis Jesus,³ O. Atramentov,⁴⁹ C. Avila,⁸ F. Badaud,¹³ L. Bagby,⁵⁰ B. Baldin,⁵⁰ D. V. Bandurin,⁵⁹ P. Banerjee,²⁹ S. Banerjee,²⁹ E. Barberis,⁶³ A.-F. Barfuss,¹⁵ P. Bargassa,⁸⁰ P. Baringer,⁵⁸ J. Barreto,² J. F. Bartlett,⁵⁰ U. Bassler,¹⁸ D. Bauer,⁴³ S. Beale,⁶ A. Bean,⁵⁸ M. Begalli,³ M. Biegel,⁷³ C. Belanger-Champagne,⁴¹ L. Bellantoni,⁵⁰ A. Bellavance,⁵⁰ J. A. Benitez,⁶⁵ S. B. Beri,²⁷ G. Bernardi,¹⁷ R. Bernhard,²³ I. Bertram,⁴² M. Besançon,¹⁸ R. Beuselinck,⁴³ V. A. Bezzubov,³⁹ P. C. Bhat,⁵⁰ V. Bhatnagar,²⁷ C. Biscarat,²⁰ G. Blazey,⁵² F. Blekman,⁴³ S. Blessing,⁴⁹ D. Bloch,¹⁹ K. Bloom,⁶⁷ A. Boehnlein,⁵⁰ D. Boline,⁶² T. A. Bolton,⁵⁹ E. E. Boos,³⁸ G. Borissov,⁴² T. Bose,⁷⁷ A. Brandt,⁷⁸ R. Brock,⁶⁵ G. Brooijmans,⁷⁰ A. Bross,⁵⁰ D. Brown,⁸¹ X. B. Bu,⁷ N. J. Buchanan,⁴⁹ D. Buchholz,⁵³ M. Buehler,⁸¹ V. Buescher,²² V. Bunichev,³⁸ S. Burdin,^{42,†} T. H. Burnett,⁸² C. P. Buszello,⁴³ J. M. Butler,⁶² P. Calfayan,²⁵ S. Calvet,¹⁶ J. Cammin,⁷¹ W. Carvalho,³ B. C. K. Casey,⁵⁰ H. Castilla-Valdez,³³ S. Chakrabarti,¹⁸ D. Chakraborty,⁵² K. Chan,⁶ K. M. Chan,⁵⁵ A. Chandra,⁴⁸ F. Charles,^{19,**} E. Cheu,⁴⁵ F. Chevallier,¹⁴ D. K. Cho,⁶² S. Choi,³² B. Choudhary,²⁸ L. Christofek,⁷⁷ T. Christoudias,⁴³ S. Cihangir,⁵⁰ D. Claes,⁶⁷ J. Clutter,⁵⁸ M. Cooke,⁸⁰ W. E. Cooper,⁵⁰ M. Corcoran,⁸⁰ F. Couderc,¹⁸ M.-C. Cousinou,¹⁵ S. Crépe-Renaudin,¹⁴ V. Cuplov,⁵⁹ D. Cutts,⁷⁷ M. Ćwiok,³⁰ H. da Motta,² A. Das,⁴⁵ G. Davies,⁴³ K. De,⁷⁸ S. J. de Jong,³⁵ E. De La Cruz-Burelo,⁶⁴ C. De Oliveira Martins,³ J. D. Degenhardt,⁶⁴ F. Déliot,¹⁸ M. Demarteau,⁵⁰ R. Demina,⁷¹ D. Denisov,⁵⁰ S. P. Denisov,³⁹ S. Desai,⁵⁰ H. T. Diehl,⁵⁰ M. Diesburg,⁵⁰ A. Dominguez,⁶⁷ H. Dong,⁷² L. V. Dudko,³⁸ L. Dufloy,¹⁶ S. R. Dugad,²⁹ D. Duggan,⁴⁹ A. Duperrin,¹⁵ J. Dyer,⁶⁵ A. Dyshkant,⁵² M. Eads,⁶⁷ D. Edmunds,⁶⁵ J. Ellison,⁴⁸ V. D. Elvira,⁵⁰ Y. Enari,⁷⁷ S. Eno,⁶¹ P. Ermolov,^{38,**} H. Evans,⁵⁴ A. Evdokimov,⁷³ V. N. Evdokimov,³⁹ A. V. Ferapontov,⁵⁹ T. Ferbel,⁷¹ F. Fiedler,²⁴ F. Filthaut,³⁵ W. Fisher,⁵⁰ H. E. Fisk,⁵⁰ M. Fortner,⁵² H. Fox,⁴² S. Fu,⁵⁰ S. Fuess,⁵⁰ T. Gadfort,⁷⁰ C. F. Galea,³⁵ E. Gallas,⁵⁰ C. Garcia,⁷¹ A. Garcia-Bellido,⁸² V. Gavrilov,³⁷ P. Gay,¹³ W. Geist,¹⁹ D. Gelé,¹⁹ C. E. Gerber,⁵¹ Y. Gershtein,⁴⁹ D. Gillberg,⁶ G. Ginther,⁷¹ N. Gollub,⁴¹ B. Gómez,⁸ A. Goussiou,⁸² P. D. Grannis,⁷² H. Greenlee,⁵⁰ Z. D. Greenwood,⁶⁰ E. M. Gregores,⁴ G. Grenier,²⁰ Ph. Gris,¹³ J.-F. Grivaz,¹⁶ A. Grohsjean,²⁵ S. Grünendahl,⁵⁰ M. W. Grünewald,³⁰ F. Guo,⁷² J. Guo,⁷² G. Gutierrez,⁵⁰ P. Gutierrez,⁷⁵ A. Haas,⁷⁰ N. J. Hadley,⁶¹ P. Haefner,²⁵ S. Hagopian,⁴⁹ J. Haley,⁶⁸ I. Hall,⁶⁵ R. E. Hall,⁴⁷ L. Han,⁷ K. Harder,⁴⁴ A. Harel,⁷¹ J. M. Hauptman,⁵⁷ R. Hauser,⁶⁵ J. Hays,⁴³ T. Hebbeker,²¹ D. Hedin,⁵² J. G. Hegeman,³⁴ A. P. Heinson,⁴⁸ U. Heintz,⁶² C. Hensel,^{22,§} K. Herner,⁷² G. Hesketh,⁶³ M. D. Hildreth,⁵⁵ R. Hirosky,⁸¹ J. D. Hobbs,⁷² B. Hoeneisen,¹² H. Hoeth,²⁶ M. Hohlfeld,²² S. Hossain,⁷⁵ P. Houben,³⁴ Y. Hu,⁷² Z. Hubacek,¹⁰ V. Hynek,⁹ I. Iashvili,⁶⁹ R. Illingworth,⁵⁰ A. S. Ito,⁵⁰ S. Jabeen,⁶² M. Jaffré,¹⁶ S. Jain,⁷⁵ K. Jakobs,²³ C. Jarvis,⁶¹ R. Jesik,⁴³ K. Johns,⁴⁵ C. Johnson,⁷⁰ M. Johnson,⁵⁰ A. Jonckheere,⁵⁰ P. Jonsson,⁴³ A. Juste,⁵⁰ E. Kajfasz,¹⁵ J. M. Kalk,⁶⁰ D. Karmanov,³⁸ P. A. Kasper,⁵⁰ I. Katsanos,⁷⁰ D. Kau,⁴⁹ V. Kaushik,⁷⁸ R. Kehoe,⁷⁹ S. Kermiche,¹⁵ G. Kertzscher,⁶ N. Khalatyan,⁵⁰ A. Khanov,⁷⁶ A. Kharchilava,⁶⁹ Y. M. Kharzheev,³⁶ D. Khatidze,⁷⁰ T. J. Kim,³¹ M. H. Kirby,⁵³ M. Kirsch,²¹ B. Klima,⁵⁰ J. M. Kohli,²⁷ J.-P. Konrath,²³ A. V. Kozelov,³⁹ J. Kraus,⁶⁵ T. Kuhl,²⁴ A. Kumar,⁶⁹ A. Kupco,¹¹ T. Kurča,²⁰ V. A. Kuzmin,³⁸ J. Kvita,⁹ F. Lacroix,¹³ D. Lam,⁵⁵ S. Lammers,⁷⁰ G. Landsberg,⁷⁷ P. Lebrun,²⁰ W. M. Lee,⁵⁰ A. Leflat,³⁸ J. Lellouch,¹⁷ J. Li,⁷⁸ L. Li,⁴⁸ Q. Z. Li,⁵⁰ S. M. Lietti,⁵ J. G. R. Lima,⁵² D. Lincoln,⁵⁰ J. Linnemann,⁶⁵ V. V. Lipaev,³⁹ R. Lipton,⁵⁰ Y. Liu,⁷ Z. Liu,⁶ A. Lobodenko,⁴⁰ M. Lokajicek,¹¹ P. Love,⁴² H. J. Lubatti,⁸² R. Luna,³ A. L. Lyon,⁵⁰ A. K. A. Maciel,² D. Mackin,⁸⁰ R. J. Madaras,⁴⁶ P. Mättig,²⁶ C. Magass,²¹ A. Magerkurth,⁶⁴ P. K. Mal,⁸² H. B. Malbouisson,³ S. Malik,⁶⁷ V. L. Malyshev,³⁶ H. S. Mao,⁵⁰ Y. Maravin,⁵⁹ B. Martin,¹⁴ R. McCarthy,⁷² A. Melnitchouk,⁶⁶ L. Mendoza,⁸ P. G. Mercadante,⁵ M. Merkin,³⁸ K. W. Merritt,⁵⁰ A. Meyer,²¹ J. Meyer,^{22,§} T. Millet,²⁰ J. Mitrevski,⁷⁰ R. K. Mommsen,⁴⁴ N. K. Mondal,²⁹ R. W. Moore,⁶ T. Moulik,⁵⁸ G. S. Muanza,²⁰ M. Mulhearn,⁷⁰ O. Mundal,²² L. Mundim,³ E. Nagy,¹⁵ M. Naimuddin,⁵⁰ M. Narain,⁷⁷ N. A. Naumann,³⁵ H. A. Neal,⁶⁴ J. P. Negret,⁸ P. Neustroev,⁴⁰ H. Nilsen,²³ H. Nogima,³ S. F. Novaes,⁵ T. Nunnemann,²⁵ V. O'Dell,⁵⁰ D. C. O'Neil,⁶ G. Obrant,⁴⁰ C. Ochando,¹⁶ D. Onoprienko,⁵⁹ N. Oshima,⁵⁰ N. Osman,⁴³ J. Osta,⁵⁵ R. Otec,¹⁰ G. J. Otero y Garzón,⁵⁰ M. Owen,⁴⁴ P. Padley,⁸⁰ M. Pangilinan,⁷⁷ N. Parashar,⁵⁶ S.-J. Park,^{22,§} S. K. Park,³¹ J. Parsons,⁷⁰ R. Partridge,⁷⁷ N. Parua,⁵⁴ A. Patwa,⁷³ G. Pawloski,⁸⁰ B. Penning,²³ M. Perfilov,³⁸ K. Peters,⁴⁴ Y. Peters,²⁶ P. Pétroff,¹⁶ M. Petteni,⁴³ R. Piegaia,¹ J. Piper,⁶⁵ M.-A. Pleier,²² P. L. M. Podesta-Lerma,^{33,‡} V. M. Podstavkov,⁵⁰ Y. Pogorelov,⁵⁵ M.-E. Pol,² P. Polozov,³⁷ B. G. Pope,⁶⁵ A. V. Popov,³⁹ C. Potter,⁶ W. L. Prado da Silva,³ H. B. Prosper,⁴⁹ S. Protopopescu,⁷³ J. Qian,⁶⁴ A. Quadt,^{22,§} B. Quinn,⁶⁶ A. Rakitine,⁴² M. S. Rangel,² K. Ranjan,²⁸ P. N. Ratoff,⁴² P. Renkel,⁷⁹ S. Reucroft,⁶³ P. Rich,⁴⁴ J. Rieger,⁵⁴ M. Rijssenbeek,⁷² I. Ripp-Baudot,¹⁹ F. Rizatdinova,⁷⁶ S. Robinson,⁴³ R. F. Rodrigues,³

M. Rominsky,⁷⁵ C. Royon,¹⁸ P. Rubinov,⁵⁰ R. Ruchti,⁵⁵ G. Safronov,³⁷ G. Sajot,¹⁴ A. Sánchez-Hernández,³³
M. P. Sanders,¹⁷ B. Sanghi,⁵⁰ G. Savage,⁵⁰ L. Sawyer,⁶⁰ T. Scanlon,⁴³ D. Schaile,²⁵ R. D. Schamberger,⁷² Y. Scheglov,⁴⁰
H. Schellman,⁵³ T. Schliephake,²⁶ C. Schwanenberger,⁴⁴ A. Schwartzman,⁶⁸ R. Schwienhorst,⁶⁵ J. Sekaric,⁴⁹
H. Severini,⁷⁵ E. Shabalina,⁵¹ M. Shamim,⁵⁹ V. Shary,¹⁸ A. A. Shchukin,³⁹ R. K. Shivpuri,²⁸ V. Siccaldi,¹⁹ V. Simak,¹⁰
V. Sirotenko,⁵⁰ P. Skubic,⁷⁵ P. Slattery,⁷¹ D. Smirnov,⁵⁵ G. R. Snow,⁶⁷ J. Snow,⁷⁴ S. Snyder,⁷³ S. Söldner-Rembold,⁴⁴
L. Sonnenschein,¹⁷ A. Sopczak,⁴² M. Sosebee,⁷⁸ K. Soustruznik,⁹ B. Spurlock,⁷⁸ J. Stark,¹⁴ J. Steele,⁶⁰ V. Stolin,³⁷
D. A. Stoyanova,³⁹ J. Strandberg,⁶⁴ S. Strandberg,⁴¹ M. A. Strang,⁶⁹ E. Strauss,⁷² M. Strauss,⁷⁵ R. Ströhmer,²⁵ D. Strom,⁵³
L. Stutte,⁵⁰ S. Sumowidagdo,⁴⁹ P. Svoisky,⁵⁵ A. Sznajder,³ P. Tamburello,⁴⁵ A. Tanasijczuk,¹ W. Taylor,⁶ B. Tiller,²⁵
F. Tissandier,¹³ M. Titov,¹⁸ V. V. Tokmenin,³⁶ T. Toole,⁶¹ I. Torchiani,²³ T. Trefzger,²⁴ D. Tsybychev,⁷² B. Tuchming,¹⁸
C. Tully,⁶⁸ P. M. Tuts,⁷⁰ R. Unalan,⁶⁵ L. Uvarov,⁴⁰ S. Uvarov,⁴⁰ S. Uzunyan,⁵² B. Vachon,⁶ P. J. van den Berg,³⁴
R. Van Kooten,⁵⁴ W. M. van Leeuwen,³⁴ N. Varelas,⁵¹ E. W. Varnes,⁴⁵ I. A. Vasilyev,³⁹ M. Vaupel,²⁶ P. Verdier,²⁰
L. S. Vertogradov,³⁶ M. Verzocchi,⁵⁰ F. Villeneuve-Seguier,⁴³ P. Vint,⁴³ P. Vokac,¹⁰ E. Von Toerne,⁵⁹ M. Voutilainen,^{68,II}
R. Wagner,⁶⁸ H. D. Wahl,⁴⁹ L. Wang,⁶¹ M. H. L. S. Wang,⁵⁰ J. Warchol,⁵⁵ G. Watts,⁸² M. Wayne,⁵⁵ G. Weber,²⁴
M. Weber,⁵⁰ L. Welty-Rieger,⁵⁴ A. Wenger,^{23,II} N. Wermes,²² M. Wetstein,⁶¹ A. White,⁷⁸ D. Wicke,²⁶ G. W. Wilson,⁵⁸
S. J. Wimpenny,⁴⁸ M. Wobisch,⁶⁰ D. R. Wood,⁶³ T. R. Wyatt,⁴⁴ Y. Xie,⁷⁷ S. Yacoub,⁵³ R. Yamada,⁵⁰ T. Yasuda,⁵⁰
Y. A. Yatsunenko,³⁶ H. Yin,⁷ K. Yip,⁷³ H. D. Yoo,⁷⁷ S. W. Youn,⁵³ J. Yu,⁷⁸ C. Zeitnitz,²⁶ T. Zhao,⁸² B. Zhou,⁶⁴ J. Zhu,⁷²
M. Zielinski,⁷¹ D. Zieminska,⁵⁴ A. Zieminski,^{54,*} L. Zivkovic,⁷⁰ V. Zutshi,⁵² and E. G. Zverev³⁸

(D0 Collaboration)

¹Universidad de Buenos Aires, Buenos Aires, Argentina²LAFEX, Centro Brasileiro de Pesquisas Físicas, Rio de Janeiro, Brazil³Universidade do Estado do Rio de Janeiro, Rio de Janeiro, Brazil⁴Universidade Federal do ABC, Santo André, Brazil⁵Instituto de Física Teórica, Universidade Estadual Paulista, São Paulo, Brazil⁶University of Alberta, Edmonton, Alberta, Canada,

Simon Fraser University, Burnaby, British Columbia, Canada,

York University, Toronto, Ontario, Canada,

and McGill University, Montreal, Quebec, Canada

⁷University of Science and Technology of China, Hefei, People's Republic of China⁸Universidad de los Andes, Bogotá, Colombia⁹Center for Particle Physics, Charles University, Prague, Czech Republic¹⁰Czech Technical University, Prague, Czech Republic¹¹Center for Particle Physics, Institute of Physics, Academy of Sciences of the Czech Republic, Prague, Czech Republic¹²Universidad San Francisco de Quito, Quito, Ecuador¹³LPC, Univ Blaise Pascal, CNRS/IN2P3, Clermont, France¹⁴LPSC, Université Joseph Fourier Grenoble 1, CNRS/IN2P3, Institut National Polytechnique de Grenoble, France¹⁵CPPM, Aix-Marseille Université, CNRS/IN2P3, Marseille, France¹⁶LAL, Univ Paris-Sud, IN2P3/CNRS, Orsay, France¹⁷LPNHE, IN2P3/CNRS, Universités Paris VI and VII, Paris, France¹⁸DAPNIA/Service de Physique des Particules, CEA, Saclay, France¹⁹IPHC, Université Louis Pasteur et Université de Haute Alsace, CNRS/IN2P3, Strasbourg, France²⁰IPNL, Université Lyon 1, CNRS/IN2P3, Villeurbanne, France and Université de Lyon, Lyon, France²¹III. Physikalisches Institut A, RWTH Aachen University, Aachen, Germany²²Physikalisches Institut, Universität Bonn, Bonn, Germany²³Physikalisches Institut, Universität Freiburg, Freiburg, Germany²⁴Institut für Physik, Universität Mainz, Mainz, Germany²⁵Ludwig-Maximilians-Universität München, München, Germany²⁶Fachbereich Physik, University of Wuppertal, Wuppertal, Germany²⁷Panjab University, Chandigarh, India²⁸Delhi University, Delhi, India²⁹Tata Institute of Fundamental Research, Mumbai, India³⁰University College Dublin, Dublin, Ireland³¹Korea Detector Laboratory, Korea University, Seoul, Korea³²SungKyunKwan University, Suwon, Korea³³CINVESTAV, Mexico City, Mexico³⁴FOM-Institute NIKHEF and University of Amsterdam/NIKHEF, Amsterdam, The Netherlands

- ³⁵Radboud University Nijmegen/NIKHEF, Nijmegen, The Netherlands
³⁶Joint Institute for Nuclear Research, Dubna, Russia
³⁷Institute for Theoretical and Experimental Physics, Moscow, Russia
³⁸Moscow State University, Moscow, Russia
³⁹Institute for High Energy Physics, Protvino, Russia
⁴⁰Petersburg Nuclear Physics Institute, St. Petersburg, Russia
⁴¹Lund University, Lund, Sweden,
 Royal Institute of Technology and Stockholm University, Stockholm, Sweden,
 and Uppsala University, Uppsala, Sweden
⁴²Lancaster University, Lancaster, United Kingdom
⁴³Imperial College, London, United Kingdom
⁴⁴University of Manchester, Manchester, United Kingdom
⁴⁵University of Arizona, Tucson, Arizona 85721, USA
⁴⁶Lawrence Berkeley National Laboratory and University of California, Berkeley, California 94720, USA
⁴⁷California State University, Fresno, California 93740, USA
⁴⁸University of California, Riverside, California 92521, USA
⁴⁹Florida State University, Tallahassee, Florida 32306, USA
⁵⁰Fermi National Accelerator Laboratory, Batavia, Illinois 60510, USA
⁵¹University of Illinois at Chicago, Chicago, Illinois 60607, USA
⁵²Northern Illinois University, DeKalb, Illinois 60115, USA
⁵³Northwestern University, Evanston, Illinois 60208, USA
⁵⁴Indiana University, Bloomington, Indiana 47405, USA
⁵⁵University of Notre Dame, Notre Dame, Indiana 46556, USA
⁵⁶Purdue University Calumet, Hammond, Indiana 46323, USA
⁵⁷Iowa State University, Ames, Iowa 50011, USA
⁵⁸University of Kansas, Lawrence, Kansas 66045, USA
⁵⁹Kansas State University, Manhattan, Kansas 66506, USA
⁶⁰Louisiana Tech University, Ruston, Louisiana 71272, USA
⁶¹University of Maryland, College Park, Maryland 20742, USA
⁶²Boston University, Boston, Massachusetts 02215, USA
⁶³Northeastern University, Boston, Massachusetts 02115, USA
⁶⁴University of Michigan, Ann Arbor, Michigan 48109, USA
⁶⁵Michigan State University, East Lansing, Michigan 48824, USA
⁶⁶University of Mississippi, University, Mississippi 38677, USA
⁶⁷University of Nebraska, Lincoln, Nebraska 68588, USA
⁶⁸Princeton University, Princeton, New Jersey 08544, USA
⁶⁹State University of New York, Buffalo, New York 14260, USA
⁷⁰Columbia University, New York, New York 10027, USA
⁷¹University of Rochester, Rochester, New York 14627, USA
⁷²State University of New York, Stony Brook, New York 11794, USA
⁷³Brookhaven National Laboratory, Upton, New York 11973, USA
⁷⁴Langston University, Langston, Oklahoma 73050, USA
⁷⁵University of Oklahoma, Norman, Oklahoma 73019, USA
⁷⁶Oklahoma State University, Stillwater, Oklahoma 74078, USA
⁷⁷Brown University, Providence, Rhode Island 02912, USA
⁷⁸University of Texas, Arlington, Texas 76019, USA
⁷⁹Southern Methodist University, Dallas, Texas 75275, USA
⁸⁰Rice University, Houston, Texas 77005, USA
⁸¹University of Virginia, Charlottesville, Virginia 22901, USA
⁸²University of Washington, Seattle, Washington 98195, USA

(Received 8 July 2008; revised manuscript received 20 April 2009; published 14 May 2009)

We describe a search for production of a charged Higgs boson, $q\bar{q}' \rightarrow H^+$, reconstructed in the $t\bar{b}$ final state in the mass range $180 \leq M_{H^+} \leq 300$ GeV. The search was undertaken at the Fermilab Tevatron collider with a center-of-mass energy $\sqrt{s} = 1.96$ TeV and uses 0.9 fb^{-1} of data collected with the D0 detector. We find no evidence for charged Higgs boson production and set upper limits on the production cross section in the types I, II, and III two-Higgs-doublet models (2HDMs). An excluded region in the $(M_{H^+}, \tan\beta)$ plane for type I 2HDM is presented.

In the standard model (SM), one $SU(2)$ doublet induces electroweak symmetry breaking, which leads to a single elementary scalar particle: the neutral Higgs boson. Two $SU(2)$ doublets perform the task of electroweak symmetry breaking in two-Higgs-doublet models (2HDMs) [1]. This leads to five physical Higgs bosons among which two carry charge. Hence the discovery of a charged Higgs boson would be unambiguous evidence of new physics beyond the SM. Various types of 2HDMs are distinguished by their strategy for avoiding flavor-changing neutral currents (FCNCs). In the type I 2HDM, only one of these doublets couples to fermions. In the type II 2HDM, a symmetry is imposed so that one doublet couples to up-type fermions and the other couples to down-type fermions; an approach used in minimal supersymmetry extensions [1]. In type III 2HDMs, both doublets couple to fermions, no symmetry is imposed and FCNCs are avoided by other methods. For example, in one type III model, FCNCs are suppressed by the small mass of the first and second generation quarks [2]. Searches for charged Higgs bosons will be very important at the LHC experiments, where studies of their couplings in each possible decay mode can be used to distinguish between the different models predicting their existence [3].

In this Letter we present the first search for a charged Higgs boson (H^+) directly produced by quark-antiquark annihilation, and decaying into the $t\bar{b}$ [4] final state, in the $180 \leq M_{H^+} \leq 300$ GeV mass range. In most models this decay dominates for large regions of parameter space when the H^+ mass (M_{H^+}) is greater than the mass of the top quark (m_t). Exploring the mass range $M_{H^+} > m_t$ is complementary to previous Tevatron searches [5] that have been performed in top-quark decays for the $M_{H^+} < m_t$ region. We analyze 0.9 fb^{-1} of data from $p\bar{p}$ collisions at a center-of-mass energy of $\sqrt{s} = 1.96$ TeV recorded from August 2002 to December 2006 using the D0 detector [6]. Since the D0 single top-quark analysis [7] reconstructs precisely the same final state in the s -channel $W^+ \rightarrow t\bar{b}$ process, we use the data set from that search.

Direct searches for a charged Higgs boson have been performed at the CERN e^+e^- collider (LEP) [8] and the Fermilab Tevatron collider [5], while indirect searches have been undertaken at the B factories [9,10]. No evidence for H^+ has been found so far. Limits on the charged Higgs boson mass and the ratio of vacuum expectation values of the two Higgs fields ($\tan\beta$) are typically calculated in the context of the type II 2HDM [11]. The combined results from the LEP experiments and those from B factories yield $M_{H^+} > 78.6$ GeV [11] and $M_{H^+} > 295$ GeV [9], respectively, at the 95% C.L. and assuming type II 2HDM.

The charged Higgs Yukawa couplings carry information about new physics beyond the SM and it has been noted that 2HDM couplings in types I and II 2HDM can be quite large [12]. For a type III 2HDM, large contributions from

heavy quark-antiquark annihilation can be expected if the top-quark-charm-quark mixing parameter (ξ_{tc}^U) is large [2]. In many models, if $M_{H^+} > m_t$, then the branching fraction of the charged Higgs boson to $t\bar{b}$ is of order unity, owing to the mass dependence of the couplings and the large top-quark mass.

We use the program COMPHEP [13] to simulate charged Higgs boson production and selected decay $q\bar{q}' \rightarrow H^+ \rightarrow t\bar{b} \rightarrow W^+ b\bar{b} \rightarrow \ell^+ \nu b\bar{b}$ where ℓ represents an electron or muon. This is done for seven M_{H^+} values ranging from 180 to 300 GeV. The lower mass value is dictated by the kinematics of the decay $H^+ \rightarrow t\bar{b}$ which requires $M_{H^+} > m_t + m_b$, where m_b is the mass of the bottom quark. The upper mass value is chosen based on the fact that, in this mass range, the production cross section decreases by approximately an order of magnitude for any of the models considered. The couplings are set to produce pure chiral state samples that are combined in different proportions to simulate the desired 2HDM type. The size of the interference term proportional to the product of the left and right-handed couplings is considered negligible. The size of this interference term is of order 1% of the total amplitude in the $\tan\beta < 30$ region for the type II 2HDM, much less than 1% for the type I 2HDM and nonrelevant for a type III 2HDM. Each choice of couplings determines the total width, Γ_{H^+} , and the initial-state quark flavor composition. This quark flavor composition of the signal samples is determined by the value of the element $|V_{ij}|$ of the Cabibbo-Kobayashi-Maskawa (CKM) matrix [14] and the CTEQ6L1 parton distribution functions (PDFs) [15]. In these simulated signal samples, Γ_{H^+} ranges from approximately 4 GeV for $M_{H^+} = 180$ to 9 GeV for $M_{H^+} = 300$ GeV.

In order to simulate the kinematic distributions of a particular model, the left-handed and right-handed signal samples are combined with event weights equal to the fraction of the production cross section associated with the left-handed or right-handed coupling contribution. The type II 2HDM couplings for right-handed (R) and left-handed (L) chiral states are $V_{CKM}^{qq'} g m_{q'} \tan\beta / (\sqrt{2} M_W)$ and $V_{CKM}^{qq'} g m_q \cot\beta / (\sqrt{2} M_W)$, where $V_{CKM}^{qq'}$ is the CKM matrix element, $m_q/m_{q'}$ the up/down-type quark mass, M_W the mass of the W boson and g the SM weak coupling constant. The $R(L)$ couplings in type I and III 2HDMs are $V_{qq'} g m_{q'} \tan\beta / (\sqrt{2} M_W)$ ($-V_{qq'} g m_q \tan\beta / (\sqrt{2} M_W)$) and $-(V_{CKM} \hat{Y}_D)_{qq'}$ ($(\hat{Y}_U^\dagger V_{CKM})_{qq'}$), where $\hat{Y}_{ij}^{U,D} = \xi \sqrt{2 m_i m_j} / v$, v is the vacuum expectation value and ξ is taken as a free parameter of the model. For the simulation of type I 2HDM, left-handed and right-handed samples are added in equal proportion. For the simulation of type II 2HDM, signal samples are combined to simulate four $\tan\beta$ values or ranges: $\tan\beta < 0.1$, $\tan\beta = 1$, $\tan\beta = 5$, and $\tan\beta > 10$. The type I 2HDM and $\tan\beta = 1$ type II models share the same left/right-handed proportions. For the

type III 2HDM as described in [2], quark-antiquark annihilation is dominated by right-handed couplings. This model is simulated using the same proportions of left-handed and right-handed samples as used to simulate the $\tan\beta > 10$ type II model. This approach provides an adequate simulation of signal event kinematics only for model parameter values that result in a charged Higgs width comparable or smaller than the experimental mass resolution of $\mathcal{O}(10)$ GeV.

Background contributions from $W + \text{jets}$ and top-quark pair ($t\bar{t}$) production are modeled using the ALPGEN Monte Carlo (MC) event generator [16]. The single top-quark samples are generated with the SINGLETOP [17] MC event generator. For both samples, we assume a top-quark mass of 175 GeV and use the CTEQ6L1 PDFs. After generation, the events are passed through a GEANT-based simulation [18] of the D0 detector and, subsequently, through standard reconstruction procedures that correct differences between the simulation and data.

Multijet events can mimic the signal when a jet is misidentified as an electron or when a heavy flavor hadron in a jet decays to a muon that satisfies the isolation criteria. We model these background sources using data events that contain either an object that satisfies all electron identification criteria but fails the selection on the seven-variable electromagnetic-object-likelihood, or a muon that satisfies all identification criteria (including $\Delta\mathcal{R}(\text{muon}, \text{jet}) > 0.5$) but fails track and energy isolation criteria. These event samples are normalized to the data, together with the $W + \text{jets}$ samples, before b tagging is applied [7].

We search for charged Higgs bosons in the $H^+ \rightarrow t\bar{b} \rightarrow \ell^+ \nu b\bar{b}$ final state, and hence require that events satisfy triggers with a jet and an electron or muon. Selections that are identical to the two-jet analysis channel for the D0 single top-quark analysis [7] are imposed on each observable in the data, background and charged Higgs boson signal samples to select events with $t\bar{b}$ final state signatures. Events are required to have a primary vertex with three or more tracks attached and a lepton originating from the primary vertex [7]. The electron (muon) channel selection requires only one isolated electron (muon) with $E_T > 15$ ($p_T > 18$) GeV within the pseudorapidity region $|\eta| < 1.1$ (2.0). Events with two isolated leptons are rejected. For both channels, events are required to have missing transverse energy within $15 < \cancel{E}_T < 200$ GeV. We require that events have exactly two jets, with the highest p_T jet satisfying $p_T > 25$ GeV and $|\eta| < 2.5$, and the second jet satisfying $p_T > 20$ GeV and $|\eta| < 3.4$.

Since both jets of the signal events are b jets, we select data events having one or two jets identified as such via a neural network-based tagging algorithm [19]. MC simulated events are weighted using a b -tag probability derived from data. The signal acceptances after the complete selection increase monotonically in the mass range $200 < M_{H^+} < 300$ GeV, for example, from $(0.48 \pm 0.06)\%$ to

$(1.24 \pm 0.20)\%$ for $\tan\beta < 0.1$, statistical and systematic uncertainties included. The signal acceptances for a given M_{H^+} decreases by at most 0.12% with increasing $\tan\beta$.

A distinctive feature of signal events is the large mass of the charged Higgs boson. We therefore use the reconstructed invariant mass of the top and bottom quark system as the discriminating variable for the charged Higgs signal. We define this variable as the invariant mass $M(\text{jet1}, \text{jet2}, W)$. In the reconstruction of the W boson, there are up to two possible solutions for the neutrino momentum component along the beam axis (p_z). In these cases, the solution with the smallest absolute value of the p_z momentum is chosen. Figure 1 shows the $M(\text{jet1}, \text{jet2}, W)$ distribution after selection, with an example signal normalized to the production cross section for a type I 2HDM [2] and for three different mass values.

The data yield for all analysis channels combined amounts to 697 events, after the complete selection. Similarly, for the sum of all background sources, the total expected yield is 721 ± 42 . For the separate background sources, the yields are 531 ± 111 for $W + \text{jets}$, 95 ± 19 for multijets, 59 ± 14 for $t\bar{t}$, and 36 ± 7 for the single top background. Anticorrelation between the $W + \text{jets}$ and multijets backgrounds results in a total background uncertainty smaller than the separate background uncertainties added in quadrature.

The systematic uncertainties on the signal and background rates are estimated using the methods described

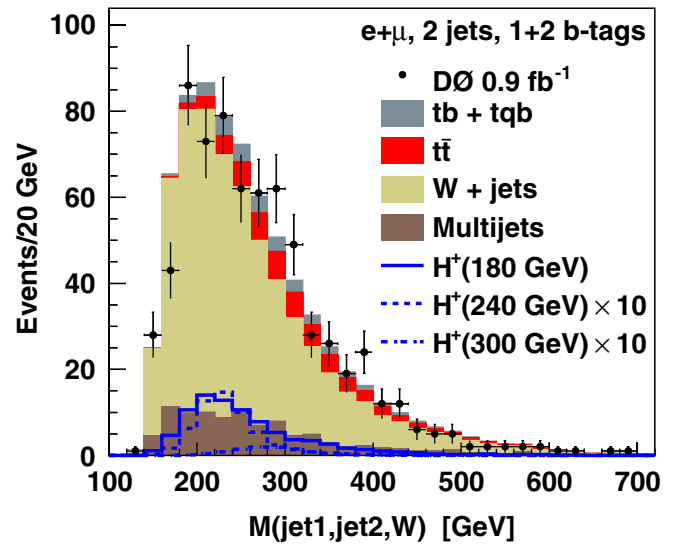


FIG. 1 (color online). Distribution of the discriminating variable, $M(\text{jet1}, \text{jet2}, W)$, for the signal, background model and data, for the combined electron and muon channels with exactly two jets and with one or two b tags. The signal distributions correspond to a type I 2HDM for charged Higgs boson masses 180, 240, 300 GeV, and are normalized according to the production cross section presented in Ref. [2] scaled by factors of 1, 10, and 10, respectively. The data are compatible with the background model, with a $\chi^2 p$ value of 0.993.

TABLE I. Observed limits on the production cross section (in pb) times branching fraction $\sigma(q\bar{q}' \rightarrow H^+) \times \mathcal{B}(H^+ \rightarrow t\bar{b})$. The expected limits are shown in parenthesis for comparison. These limits apply to the type II 2HDM. The limits obtained for $\tan\beta = 1$ and $\tan\beta > 10$ are also valid for type I and type III 2HDMs, respectively. Limits shown in square brackets are only valid for the general production of a charged scalar via a purely left-handed coupling with width smaller than the experimental resolution. These limits are not valid for the production of a charged Higgs boson in type II 2HDM since the charged Higgs width is expected to be larger than the experimental resolution.

M_{H^+} (GeV)	$\tan\beta < 0.1$	$\tan\beta = 1$	$\tan\beta = 5$	$\tan\beta > 10$
180	12.9 (11.4)	14.3 (12.2)	13.7 (11.7)	13.7 (12.2)
200	[5.9 (9.6)]	6.3 (9.9)	6.5 (10.0)	6.5 (10.0)
220	[2.9 (4.2)]	3.0 (4.4)	3.0 (4.5)	3.0 (4.5)
240	[2.3 (3.1)]	2.4 (3.3)	2.6 (3.5)	2.6 (3.5)
260	[3.0 (2.8)]	3.0 (2.9)	3.0 (3.0)	3.0 (3.0)
280	[4.0 (2.6)]	4.2 (2.7)	4.5 (2.9)	4.5 (2.9)
300	[4.5 (2.4)]	4.7 (2.4)	4.9 (2.5)	4.9 (2.5)

in Ref. [7]. Dominant sources of systematic uncertainty arise from the jet energy scale correction (1%–20%), the b -tag rates applied to MC events (12%–17% for double-tagged events), normalization of the $t\bar{t}$ background to theory (18%), and normalization of the W + jets and multijet backgrounds to data (17%–27%). For the H^+ signal, the uncertainty on the model-dependent proportion of initial-state parton flavor contribution plays a dominant role. Simulated signal events with different exclusive initial-state quark combinations are used to assess the latter source of uncertainty. A value of 10% is assigned based on the variations in the expected cross section from simulated signal samples each generated with a single initial-state parton-flavor combination: $u\bar{d}$, $u\bar{s}$, $u\bar{b}$, $c\bar{d}$, $c\bar{s}$, and $c\bar{b}$.

We observe no excess of data over background and proceed to set upper limits on H^+ boson production. We construct a binned likelihood function and use Bayesian statistics to calculate upper limits on the signal production cross section times the branching fraction ($\sigma \times \mathcal{B}$) to the $t\bar{b}$ final state. A flat prior is used for nonnegative values of the signal cross section; it is set to zero for negative values. All sources of systematic uncertainty and their correlations are taken into account in calculating $\sigma \times \mathcal{B}$ upper limits for different 2HDM types at the 95% C.L. At the level of precision reported, the observed limits are insensitive to changes in top mass in the range $170 < m_t < 175$ GeV. The observed and expected $\sigma \times \mathcal{B}$ limits are reported in Table I.

The $\sigma \times \mathcal{B}$ upper limits obtained are compared to the expected signal cross section in the type I 2HDM to exclude a region of the M_{H^+} and $\tan\beta$ parameter space, shown in Fig. 2. The analysis sensitivity is currently not sufficient to exclude regions of $\tan\beta < 100$ in the type II 2HDM. In a type III 2HDM [2], the charged Higgs boson

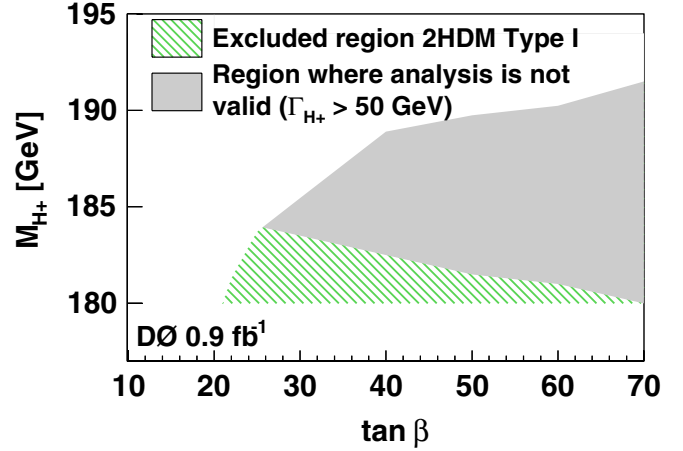


FIG. 2 (color online). The 95% C.L. excluded region in the M_{H^+} vs $\tan\beta$ space for type I 2HDM. The region for which $\Gamma_{H^+} > 50$ GeV indicates the approximate area where the charged Higgs width is significantly larger than the detector resolution and hence the analysis is not valid.

width depends quadratically on the mixing parameter ξ . This limits our ability to exclude regions in the M_{H^+} and ξ parameter space.

In summary, we have performed the first direct search for the production of charged Higgs bosons in the reaction $q\bar{q}' \rightarrow H^+ \rightarrow t\bar{b}$ and we have presented limits on the production cross section times branching fraction for types I, II and III 2HDMs in the mass range $180 \leq M_{H^+} \leq 300$ GeV. A region in the M_{H^+} vs $\tan\beta$ plane has been excluded at the 95% C.L. for type I 2HDMs.

We thank the staffs at Fermilab and collaborating institutions, and acknowledge support from the DOE and NSF (USA); CEA and CNRS/IN2P3 (France); FASI, Rosatom and RFBR (Russia); CNPq, FAPERJ, FAPESP and FUNDUNESP (Brazil); DAE and DST (India); Colciencias (Colombia); CONACyT (Mexico); KRF and KOSEF (Korea); CONICET and UBACyT (Argentina); FOM (The Netherlands); STFC (United Kingdom); MSMT and GACR (Czech Republic); CRC Program, CFI, NSERC and WestGrid Project (Canada); BMBF and DFG (Germany); SFI (Ireland); The Swedish Research Council (Sweden); CAS and CNSF (China); and the Alexander von Humboldt Foundation (Germany).

*Visitor from Augustana College, Sioux Falls, SD, USA.
[†]Visitor from The University of Liverpool, Liverpool, United Kingdom.
[‡]Visitor from ICN-UNAM, Mexico City, Mexico.
[§]Visitor from II. Physikalisches Institut, Georg-August-University, Göttingen, Germany.
^{||}Visitor from Helsinki Institute of Physics, Helsinki, Finland.
[¶]Visitor from Universität Zürich, Zürich, Switzerland.

- **Deceased.
- [1] J. Gunion *et al.*, *The Higgs Hunter's Guide*, Frontiers in Physics (Westview Press, Boulder, CO, 2000).
- [2] H.-J. He and C.-P. Yuan, Phys. Rev. Lett. **83**, 28 (1999).
- [3] K. A. Assamagan and N. Gollub, Eur. Phys. J. C **39**, 25 (2005); S. Lowette, Czech. J. Phys. **55**, B831 (2005).
- [4] We use the H^+ notation to refer to both H^+ and its charge conjugate state H^- . Similarly, the $t\bar{b}$ notation is used here to represent both the $t\bar{b}$ state and its charge conjugate state $\bar{t}b$.
- [5] B. Abbott *et al.* (D0 Collaboration), Phys. Rev. Lett. **82**, 4975 (1999); V.M. Abazov *et al.* (D0 Collaboration), Phys. Rev. Lett. **88**, 151803 (2002); A. Abulencia *et al.* (CDF Collaboration), Phys. Rev. Lett. **96**, 042003 (2006).
- [6] V.M. Abazov *et al.* (D0 Collaboration), Nucl. Instrum. Methods Phys. Res., Sect. A **565**, 463 (2006).
- [7] V.M. Abazov *et al.* (D0 Collaboration), Phys. Rev. Lett. **98**, 181802 (2007); V.M. Abazov *et al.* (D0 Collaboration), Phys. Rev. D **78**, 012005 (2008).
- [8] G. Abbiendi *et al.* (OPAL Collaboration), Eur. Phys. J. C **7**, 407 (1999); R. Barate *et al.* (ALEPH Collaboration), Phys. Lett. B **543**, 1 (2002); J. Abdallah *et al.* (DELPHI Collaboration), Phys. Lett. B **525**, 17 (2002); P. Achard *et al.* (L3 Collaboration), Phys. Lett. B **575**, 208 (2003).
- [9] M. Misiak *et al.*, Phys. Rev. Lett. **98**, 022002 (2007).
- [10] A.G. Akeroyd and S. Recksiegel, J. Phys. G **29**, 2311 (2003).
- [11] W.-M. Yao *et al.*, J. Phys. G **33**, 1 (2006).
- [12] D.P. Roy, Mod. Phys. Lett. A **19**, 1813 (2004).
- [13] E. Boos *et al.*, (COMPHEP Collaboration), Nucl. Instrum. Methods Phys. Res., Sect. A **534**, 250 (2004).
- [14] N. Cabibbo, Phys. Rev. Lett. **10**, 531 (1963); M. Kobayashi and K. Maskawa, Prog. Theor. Phys. **49**, 652 (1973).
- [15] J. Pumplin *et al.*, J. High Energy Phys. 07 (2002) 012.
- [16] M.L. Mangano *et al.*, J. High Energy Phys. 07 (2003) 001. We used ALPGEN version 2.05.
- [17] E. Boos *et al.*, Phys. At. Nucl. **69**, 1317 (2006).
- [18] R. Brun and F. Carminati, CERN Program Library Long Writup No. W5013, 1993.
- [19] T. Scanlon, Ph.D. thesis, University of London, 2006.